(in a system of units where the magnetic length $l_H = 1$ and $e = c$, $\omega_H = 1/m$). Such a special form of the polarization operator is because the electron – hole polarization loop in the coordinate representation is a function of $(\mathbf{r} - \mathbf{r}')$ if an external magnetic field is present.

A plasmon propagator, like $D(\omega, q)$, has the form (6). In the presence of a completely filled Landau level in $\Pi(\omega, q)$ valleys, additional energy comes into play due to the electron being transferred from an occupied valley to the same level in an empty valley, with a hole left behind. This energy has its origin in exchange effects and corresponds to a spin wave in the one-valley case. This is a neutral excitation, and one which is characterized by a momentum, despite the presence of a magnetic field. In this situation, an exchange exciton forms. At a large momentum, the electron and the hole are far apart, their interaction is negligible, and they can therefore be considered free — leading to the conclusion that their energy is the activation energy for charge excitations, the electron energy difference between the empty and occupied valleys. This energy can be calculated to give

$$\Delta = \int D(0,q)\ \exp\left(-\frac{q^2}{2}\right)\frac{\mathrm{d}^2\mathbf{q}}{(2\pi)^2} = \frac{\hbar\omega_H}{\nu}\left(\log(r_s\nu^{3/2}) + 0.277\right), \qquad (20)$$

($r_s = \sqrt{2}e^2/\omega_H l_H\sqrt{\nu}$), showing that the activation energy is approximately proportional to the magnetic field and is small in the limit of large ν. The linear behavior agrees qualitatively with the magneto-conductance measurements of the activation energy [10], but Eqn (20) greatly overestimates the activation energy — possibly because the extrapolation to relatively large r_s is itself a rather crude procedure or because factors such as a finite thickness of the 2D layer or the image force from the metal gate were not taken into account.

The energy of an exchange exciton at low momentum Q is calculated in a similar way, giving

$$\omega(Q) = J(Ql_H)^2, \quad J = 0.6613\ \frac{\omega_H}{\nu}\,. \qquad (21)$$

Thus, we see that the exchange constant J is also screening-suppressed and varies linearly with the magnetic field.

Some of the results in this paper were previously presented in Ref. [16].

Acknowledgements. This work was supported by RFBR grants 03-02-17229a and 0501-16553a.

References

1. Ando T, Fowler A B, Stern F *Rev. Mod. Phys.* **54** 437 (1982)
2. Abrahams E, Kravchenko S V, Sarachik M P *Rev. Mod. Phys.* **73** 251 (2001)
3. Pudalov V M et al. *Phys. Rev. Lett.* **88** 196404 (2002)
4. Shashkin A A et al. *Phys. Rev. B* **66** 073303 (2002)
5. Bagaev V S et al. *Pis'ma Zh. Eksp. Teor. Fiz.* **10** 309 (1969) [*JETP Lett.* **10** 195 (1969)]
6. Jeffries C D, Keldysh L V (Eds) *Electron-Hole Droplets in Semiconductors* (Modern Problems in Condensed Matter Sciences, Vol. 6) (Amsterdam: North-Holland Publ. Co., 1983)
7. Gell-Mann M, Brueckner K A *Phys. Rev.* **106** 364 (1957); Sawada K *Phys. Rev.* **106** 372 (1957); Gell-Mann M *Phys. Rev.* **106** 369 (1957)
8. Smith J L, Stiles P J *Phys. Rev. Lett.* **29** 102 (1972)
9. Okamoto T et al. *Phys. Rev. Lett.* **82** 3875 (1999)
10. Khrapai V S, Shashkin A A, Dolgopolov V T *Phys. Rev. B* **67** 113305 (2003)
11. Bychkov Yu A, Iordanskii S V, Eliashberg G M *Pis'ma Zh. Eksp. Teor. Fiz.* **33** 152 (1981) [*JETP Lett.* **33** 143 (1981)]; Kallin C, Halperin B I *Phys. Rev. B* **30** 5655 (1984)
12. Takada Y *Phys. Rev. B* **43** 5962 (1991)
13. Abrikosov A A, Gor'kov L P, Dzyaloshinskii I E *Metody Kvantovoi Teorii Polya v Statisticheskoi Fizike* (Methods of Quantum Field Theory in Statistical Physics) (Moscow: Dobrosvet, 1998) [Translated into English (New York: Dover Publ., 1975)]
14. Pudalov V M, Gershenson M E, Kojima H, in *Fundamental Problems of Mesoscopic Physics*: *Interactions and Decoherence* (NATO Sci. Ser., Ser. II, Vol. 154, Eds I V Lerner, B L Altshuler, Y Gefen) (Dordrecht: Kluwer Acad. Publ., 2004)
15. Pines D, Nozières P *The Theory of Quantum Liquids* (New York: W.A. Benjamin, 1966)
16. Iordanski S V, Kashuba A *Pis'ma Zh. Eksp. Teor. Fiz.* **76** 660 (2002) [*JETP Lett.* **76** 563 (2002)]

PACS numbers: **71.27.+a**, **71.30.+h**, 72.15.Rn

DOI: 10.1070/PU2006v049n02ABEH005923

Interaction effects in the transport and magnetotransport of two-dimensional electrons in AlGaAs/GaAs and Si/SiGe heterojunctions

E B Olshanetskii, V Renard, Z D Kvon, I V Gornyi, A I Toropov, J C Portal

1. Introduction

Localization- and interaction-induced quantum corrections to the conductivity of two-dimensional (2D) electron systems [1, 2] have been the subject of considerable study since as long as a quarter century ago. It should be noted that weak localization effects do not present any problems, and that their associated anomalous magnetoresistance very soon became a powerful tool for probing the low-temperature properties of disordered metallic systems, from thin superconducting films to near-surface 2D layers in semiconductors. Unlike this, the behavior of interaction effects remained the subject of continuous heated debate — primarily in connection with how they influence the metal – insulator transition in a 2D electron system [3]. What made things especially topical was the discovery [4] that a high-mobility 2D electron gas in silicon MOS (metal-oxide-semiconductor) transistors exhibits states whose conductivity increases anomalously with lowering the temperature, which is entirely inconsistent with theoretical expectations [1, 2]. This situation has stimulated new ideas in the theory of interaction-induced quantum corrections and has recently led to its further development in Refs [5 – 7], which identified two regimes — the diffusion one (for $T\tau/\hbar \ll 1$) and the ballistic one (for $T\tau/\hbar \gg 1$) — in the behavior of quantum corrections. Both regimes are of the same nature, i.e., are determined by single and multiple scattering from impurities and from the Friedel oscillations in their screening charge. Both mechanisms had already been know before Refs [5 – 7]. The first mechanism [1, 2] was thought to be related to the quantum corrections due to the interference of interacting electrons (see above), and the second was linked to the temperature dependence of screening due to the singularity in 2D screening near $q \approx 2k_F$ [8] and was considered to be a temperature-dependent part of the one-electron transport time, unrelated to quantum interference.

There was a series of experiments [9–12] to verify the predictions in Refs [5–7], and although a number of confirmations were obtained, none of the experiments showed the transition from one regime to the other. Nor was a study done to see experimentally how (or whether) the ballistic and quantum corrections depend on whether the primary scattering mechanism is short-range, long-range, or mixed — even though this had been shown [7] to be a very important factor in determining the behavior of the parabolic magnetoresistance due to these corrections. This talk presents experiments that used 2D electron systems (2D ESs) in an AlGaAs/GaAs/AlGaAs quantum well and in a SiGe/Si heterojunction to clarify the situation.

2. Transition from the ballistic to the diffusion regime in a 2D ES in an AlGaAs/GaAs/AlGaAs quantum well

The experiment to study the way quantum corrections change from diffusion to ballistic behavior involved a specially designed structure consisting of a high-density 2D electron gas (2D EG) in an AlGaAs/GaAs/AlGaAs quantum well doped with Si. With the concentration N_s varying in the range $(2.5-4.5)\times10^{12}$ cm^{-2} and the mobility μ between 280 and 560 cm^2 V^{-1} s^{-1}, the system under study was a low-mobility 2D EG with large values of the Fermi energy E_F ($E_F = 100-200$ meV) and the short-range potential of doped Si atoms acting as the dominant scattering mechanism. To catch the transition from $T\tau/\hbar \ll 1$ to $T\tau/\hbar \gg 1$, the maximum possible temperature range, $T = 1.4-110$ K, was covered, in which the resistance, magnetoresistance, and Hall effect were measured in detail (Fig. 1). Before proceeding to the analysis of the experiment, a close look at the theory in Refs [5, 6] is in order. According to this theory, the total quantum correction to the conductivity of a 2D ES consists of a logarithmic part and a linear part, respectively dominant at low ($T\tau/\hbar \ll 1$) and high ($T\tau/\hbar \gg 1$) temperatures. The point to note here is that in the weak interaction case, $r_s \leqslant 1$ ($r_s = E_{e-e}/E_F$), both corrections have the same sign — one for which the conductivity falls with decreasing the temperature. An interesting prediction concerns the correction $\delta\rho_{xy}$ to the classical Hall resistance ρ_H^D: its temperature dependence changes from logarithmic to hyperbolic as the temperature increases. As already noted, there exists a correction due to weak localization, along with that due to interaction. The former was excluded by conducting experiments in a magnetic field B, which completely suppresses the weak localization in our samples at $B > 5$ T. Another output from measurements in a magnetic field was the value of the Drude conductivity, which is needed for correctly comparing theory and experiment. Measurements of the temperature dependence of conductivity due to the $\Delta\sigma_{xx}^{e-e}(T)$ interaction are presented in Fig. 2a. It is clearly seen that the dependence is close to linear at high temperatures, $T > 20$ K, and becomes logarithmic for $T < 20$ K. A fairly good agreement is seen with the dependence (solid curve) predicted by the theory in Ref. [5]. We note that this agreement is obtained without the use of any fitting parameters because in the weak interaction case, the Fermi-liquid constant F_0^σ, normally used as a fitting parameter, is determined exactly [5] if the

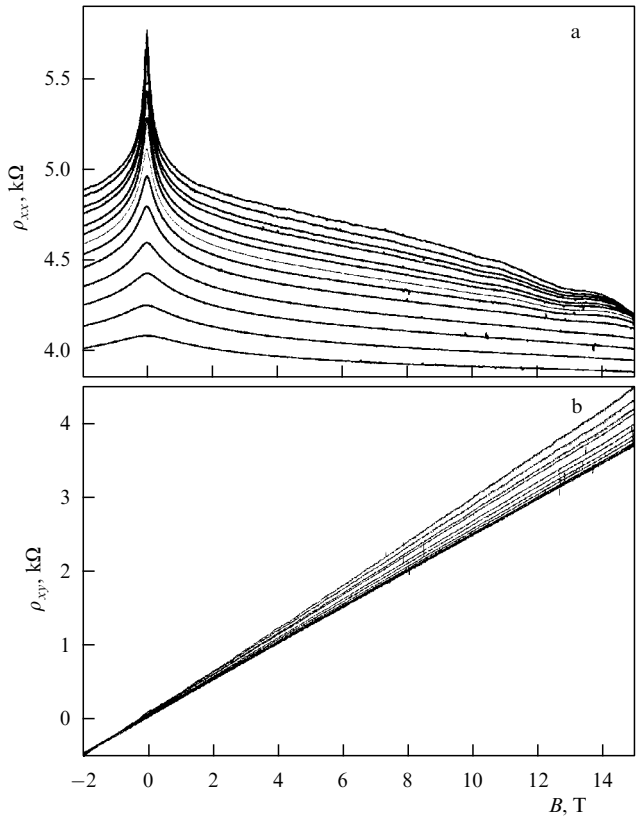

Figure 1. Resistance and magnetoresistance (a) and Hall effect (b) of an AlGaAs/GaAs/AlGaAs quantum well in the temperature range 1.4 K – 110 K.

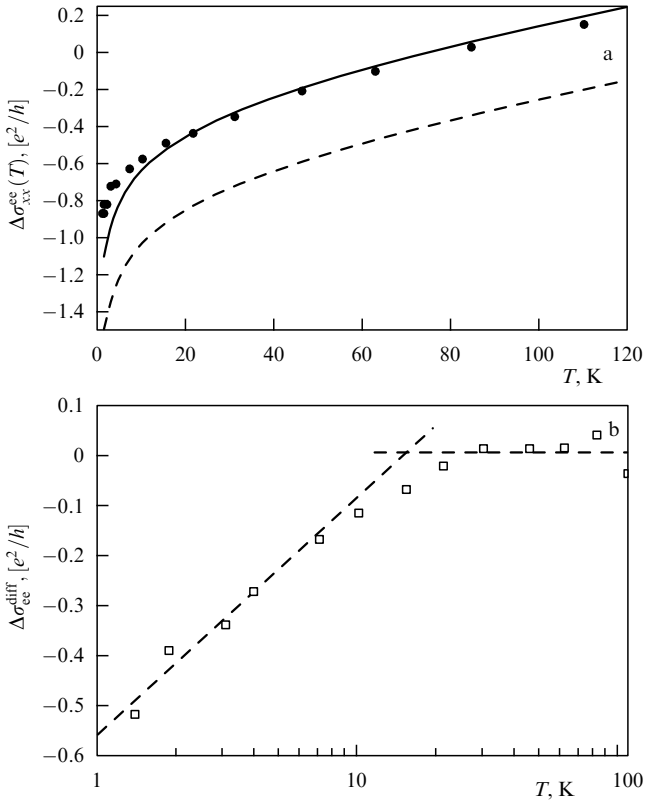

Figure 2. (a) Measured (dots) and calculated (solid line) quantum corrections due to interaction; the dashed line is for the theoretical correction calculated without account for the constant shift. (b) temperature dependence of the logarithmic correction to conductivity.

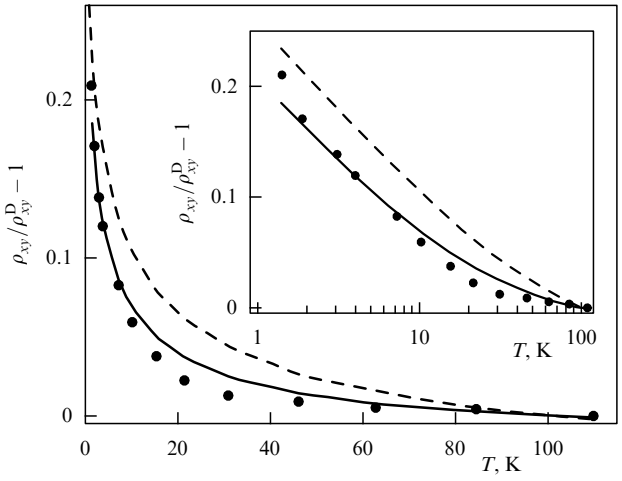

Figure 3. Temperature dependence of the Hall coefficient. Dots: experiment; dashed line: theory in Ref. [6]; solid line: the same for anisotropic electron scattering.

concentration of 2D electrons is known, which in our case was determined which it is from the Hall effect and Shubnikov–de Haas measurements on the samples studied. A specially developed technique allowed each of the interaction-induced corrections to be determined separately. Taking the logarithmic correction as an illustration, it is clearly seen from Fig. 2b that it tends to zero for $T > 20$ K. The measured and predicted corrections to the Hall resistance are compared in Fig. 3, from which it is seen that the theory in Ref. [6] explains the behavior of $\delta\rho_{xy}/\rho_{\rm H}^{\rm D}$ only qualitatively and that the experimental and theoretical dependences of $\delta\rho_{xy}/\rho_{\rm H}^{\rm D}$ on temperature disagree considerably. Still, the transition from the ballistic to diffusion regime in the behavior of the Hall effect is also clearly seen in the curves in Fig. 3, the lack of perfect agreement being most likely due to the neglect of the weak scattering anisotropy.

3. Metal–insulator transition and quantum corrections to the 2D EG conductivity in the Si/SiGe heterostructure [14]

It has been about ten years since the silicon structure metal–insulator–semiconductor (MIS) with a 2D EG was first found [4] to undergo the metal–insulator transition (MIT) forbidden in the one-parameter scaling model [15]. However, it is still unclear whether this is a phase transition. Although publications abound on the metal–insulator transition in various types of 2D ESs, there has not yet been any report of such a transition in a Si/SiGe heterojunction with a 2D EG, which is all the more unfortunate because this would allow a comparison with what has been seen on silicon MIS structures. These two systems, while totally alike in their electronic spectra, differ in the structure of the scattering potential (which is primarily short-range in silicon MISs and has a long-range component in Si/SiGe heterostructures), and hence the difference in the behavior of these systems can provide information on the role played by the dominant scattering mechanism in the electron–electron interaction.

Our experiments involved Si/SiGe heterostructures grown by molecular beam epitaxy [12], with the electron density $N_{\rm s} = (3.5-6.23) \times 10^{11}$ cm^{-2} and the maximum electron mobility $\mu = 6 \times 10^5$ cm^2 V^{-1} s^{-1}. The transport measurement employed a standard four-probe technique using a low-frequency (10 Hz) small-amplitude (0. 1 μA) ac to avoid heating effects.

The metal–insulator transition is usually observed by measuring the temperature dependence of conductivity at various concentrations of 2D electrons. The concentration in this case was varied by varying the shutter voltage. In our experiments, samples based on a 2D EG containing Si/SiGe heterojunctions were brought from their initial insulating state (which was achieved by cryostatically cooling them to the base temperature) to the metallic state (which proved to be very stable) by applying a succession of specially dosed short-duration LED pulses.

Figure 4 shows the temperature dependence of the resistance for various values of the electron concentration. The transition between the insulating, $d\rho_{xx}/dT < 0$, and metallic, $d\rho_{xx}/dT > 0$, behavior shown in this figure is the first observation of this kind in a Si/SiGe heterostructure with a 2D electron gas. At the electron concentration about 4.05×10^{11} cm^{-2}, there is a sort of boundary between these states, corresponding to the sample resistance $\approx 0.3h/e^2$. The temperature dependence of resistance corresponding to this boundary state is not monotonic (Fig. 4c). As its counterparts in other 2D systems, the observed metal–insulator transition has so far defied explanation. A theoretical analysis is possible only for states with small $r_{\rm s}$ and $\rho_{xx} \ll h/e^2$, and this is precisely where considerable progress has been made in understanding the nature of corrections to the Drude conductivity due to the electron–electron interaction. We now turn to a detailed discussion of this class of phenomena found in samples based on the Si/SiGe heterostructure with a 2D EG.

As noted above, there are two major types of corrections to the conductivity of a 2D electron system: weak localization corrections and those due to the electron–electron interaction. The weak localization correction can be written as [1]

$$\Delta\sigma_{xx}^{\rm wl} = \alpha p \, \frac{e^2}{h} \ln\left(\frac{k_{\rm B}T\tau}{\hbar}\right),$$

where the phase coherence time is assumed to vary with temperature as T^{-p}, and the amplitude α is taken to be unity for ordinary scattering.

Further, according to Ref. [5], the interaction-induced correction at arbitrary $k_{\rm B}T\tau/\hbar$ is given by

$$\Delta\sigma_{xx}^{\rm ee} = \delta\sigma_{\rm C} + 15\delta\sigma_{\rm T},$$

where

$$\delta\sigma_{\rm C} = \frac{e^2}{\pi\hbar} \, \frac{k_{\rm B}T\tau}{\hbar}\left(1 - \frac{3}{8} \, f(T\tau)\right) - \frac{e^2}{2\pi^2\hbar} \ln\left(\frac{1}{T\tau}\right)$$

and

$$\delta\sigma_{\rm T} = \frac{F_0^\sigma}{(1+F_0^\sigma)} \, \frac{e^2}{\pi\hbar} \, \frac{T\tau}{\hbar}\left(1 - \frac{3}{8} \, t\left(T\tau; F_0^\sigma\right)\right) - \left(1 - \frac{1}{F_0^\sigma}\ln\left(1+F_0^\sigma\right)\right) \frac{e^2}{2\pi^2\hbar} \ln\left(\frac{1}{T\tau}\right)$$

are the respective corrections for the interactions in the charge and triplet channels [see Ref. [5] for the exact expressions for the functions $f(T\tau)$ and $t(T\tau; F_0^\sigma)$].

We note that the expression above accounts for the fact that the electronic spectrum of Si is doubly valley-degenerate

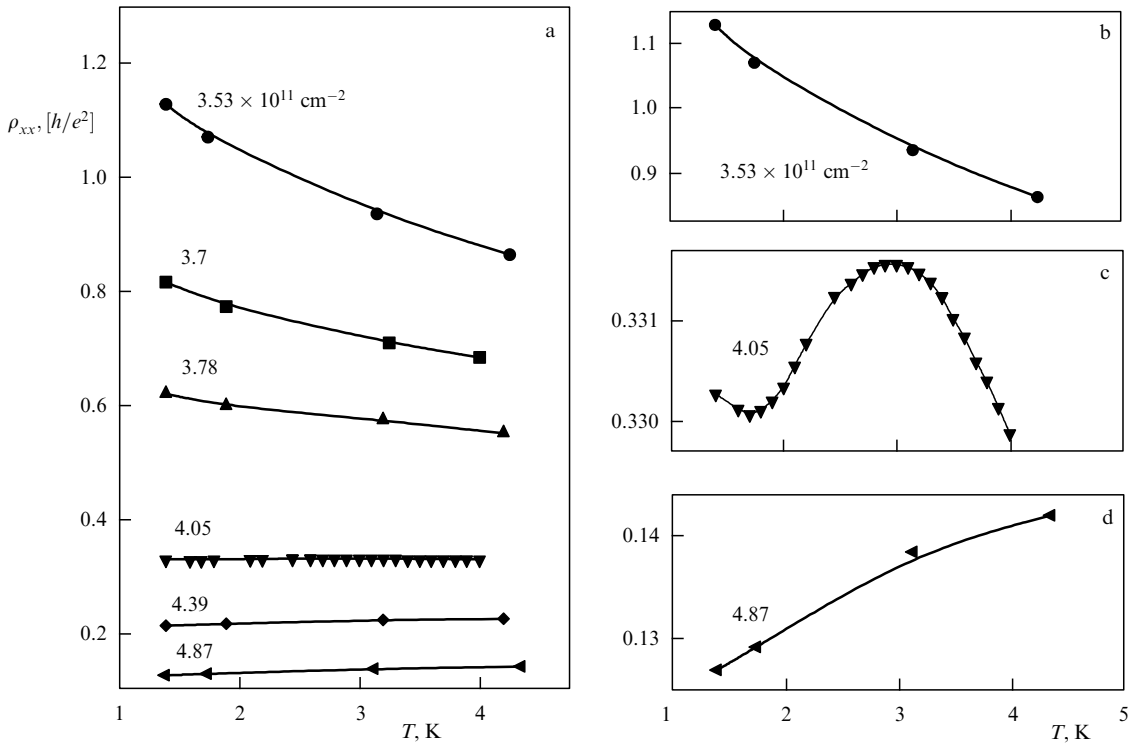

Figure 4. (a) Resistance as a function of temperature for various values of concentration. (b – d) Some of the curves of (a) shown magnified.

near the (100) surface, increasing the numerical factor in front of the triplet term from 3 to 15. In the diffusion limit, the correction due to the interaction reduces to the familiar logarithmic correction [2], whereas in the ballistic and intermediate regime, it is linear in temperature, with the sign and slope dependent on the coupling constant.

Figure 5a shows typical magnetoresistance (MR) curves measured at different temperatures after the electron concentration has been saturated to its maximum by LED radiation. In this state, the electron mobility is $\mu = 61800\ \mathrm{cm^2\,V^{-1}\,s^{-1}}$ and the electron concentration is $N_s = 6.23 \times 10^{11}\ \mathrm{cm^{-2}}$ (corresponding to $r_s \approx 6.7$). We note that for $r_s > 1$, the functional relation between the parameter r_s and the constant F_0^σ is unknown. In Fig. 5b, we show the temperature dependence of conductivity in a zero magnetic field. It is seen that the dependence is linear for $T \geqslant 1.25$ K and saturates at lower temperatures. The Drude conductivity is determined by extrapolating the linear part of the dependence to $T = 0$, and its corresponding momentum relaxation time is $\tau = 6.8 \times 10^{-12}$ s. This means that $T\tau = 0.89T$ and hence the sample under study is either in the intermediate or in the ballistic regime in the temperature range 0.4 – 2.7 K.

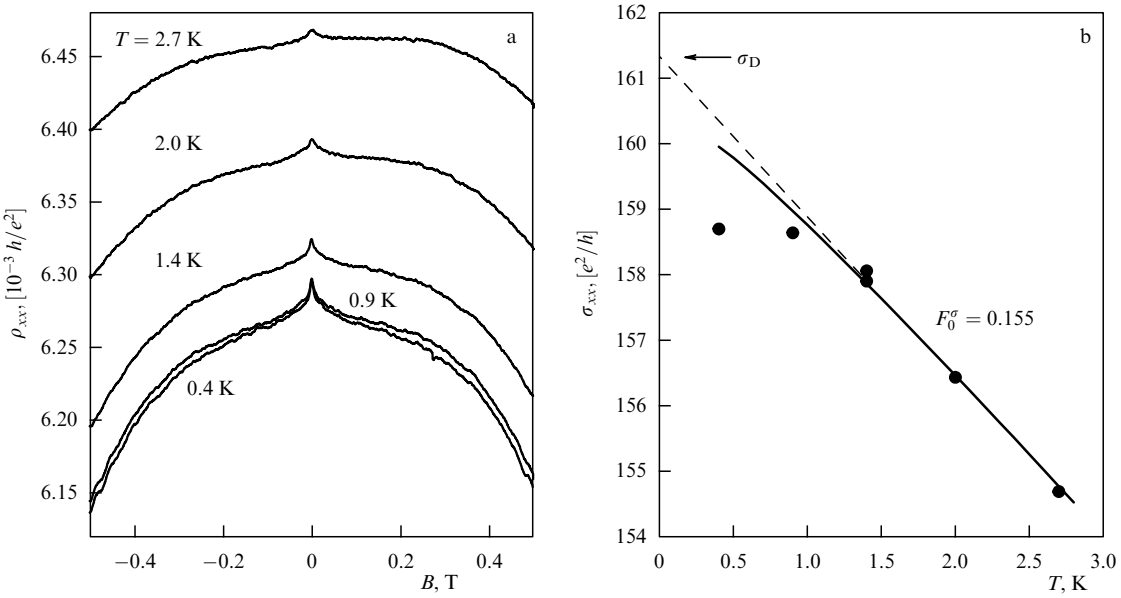

Figure 5. (a) Magnetoresistance at different temperatures. (b) Conductivity as a function of temperature for $B = 0$. Solid curve is the theoretical behavior.

The solid curve in Fig. 5b is the theoretical dependence obtained by adding the weak localization correction and that due to the interaction. It took only one fitting parameter, $F_0^\sigma = -0.155$, to fit the curve to experiment. The weak localization factor $\alpha p = 1.5$ was derived from the sample's weak-magnetic-field behavior. The value $F_0^\sigma = -0.155$ obtained by fitting turns out to be smaller than the corresponding quantities in silicon MIS structures with similar values of r_s by a surprisingly large factor of about two [10]. In our view, this results from the range difference mentioned above between the scattering potentials in these two silicon systems. According to Ref. [5], the temperature-linear interaction-induced correction to the conductivity results from the electron scattering by Friedel density oscillations due to a short-range scattering potential. This type of scattering occurs, for example, in silicon MIS structures. In our samples, the one-particle scattering time τ_q determined from the Shubnikov–de Haas amplitude turns out to be six times smaller than the momentum relaxation time, implying that both types of disorder are present in the samples. Although one might expect that the theory in Ref. [5] is inadequate for describing the experiment in this case, good agreement between theory and experiment is found for $T \geqslant 1.25$ K. One explanation may be the predominance of short-range scattering in a zero magnetic field. As regards the saturation effect observed at low temperatures, it has already been reported elsewhere [16], where intervalley scattering and the lifting of the degeneracy of a zero magnetic field were cited as possible reasons for such behavior.

We next turn to our transverse magnetoresistance results (Fig. 5a). In the diffusion regime, it is known that the zero-magnetic-field interaction-induced correction to conductivity, $\Delta\sigma_{xx}^{ee}(T)$, also retains its form in classically strong magnetic fields, leading to a negative parabolic magnetoresistance of the form $\rho_{xx}(B) = \rho_D + \rho_D^2(\mu B)^2\Delta\sigma_{xx}^{ee}(T)$ for $\omega_c\tau > 1$. Unlike the diffusion regime, the situation with the intermediate and ballistic regimes has received little attention until recently. In particular, it remained unclear whether zero-field corrections remain the same in strong magnetic fields. Recently, a new theory was proposed [7], which calculates magnetoresistance in a strong magnetic field for arbitrary values of $k_B T\tau/\hbar$. Analysis is carried out for both mixed scattering and a smoothly varying scattering potential alone, and it is shown that in both cases, the interaction leads to a parabolic MR similar to that given above except that $\Delta\sigma_{xx}^{ee}(T)$ is expressed as

$$\Delta\sigma_{xx}^{ee}(T) = -\frac{2}{\pi}\left[G_F\left(k_B T\tau/\hbar\right) - G_H\left(k_B T\tau/\hbar; F_0^\sigma\right)\right],$$

where $G_F(k_B T\tau/\hbar)$ and $G_H(k_B T\tau/\hbar; F_0^\sigma)$ are respectively the exchange and triplet contributions, whose form is dependent, among other things, on what scattering mechanism is at work in the system. The exact expressions for these functions can be found in Ref. [7].

The general features (in particular, the negative parabolic MR) seen in the experimental dependences confirm the conclusion about the presence of a magnetic-field-independent correction. Indeed, the experimental curves obtained following the suppression of the weak localization correction show a relatively flat region, which, according to Ref. [7], corresponds to the suppression at low magnetic fields of the backscattering due to the presence of a long-period scattering potential. At higher magnetic fields, the increased probability of backscattering restores the interaction, leading to negative parabolic MR.

For our sample, the condition $\omega_c\tau = 1$ is satisfied for $B = 0.16$ T, with a parabolic MR observed in classically strong fields. Moreover, all the dependences, except for the curve for $T = 0.4$ K, were measured in magnetic fields for which the influence of the Zeeman effect is negligible. Under these conditions, the predictions of the theory in Ref. [7] apply to our experiment. The dots in Fig. 6a show the resistance as a function of B^2 and in Fig. 6b show the interaction-induced corrections to conductivity, $\Delta\sigma_{xx}^{ee}(T)$, obtained from the slope of the linear portion of the dependences in Fig. 6a. Also shown in Fig. 6b are two theoretical curves from Ref. [7], one of which (*1*) is obtained on the assumption of a smooth scattering potential alone, and the other (*2*) is drawn for the

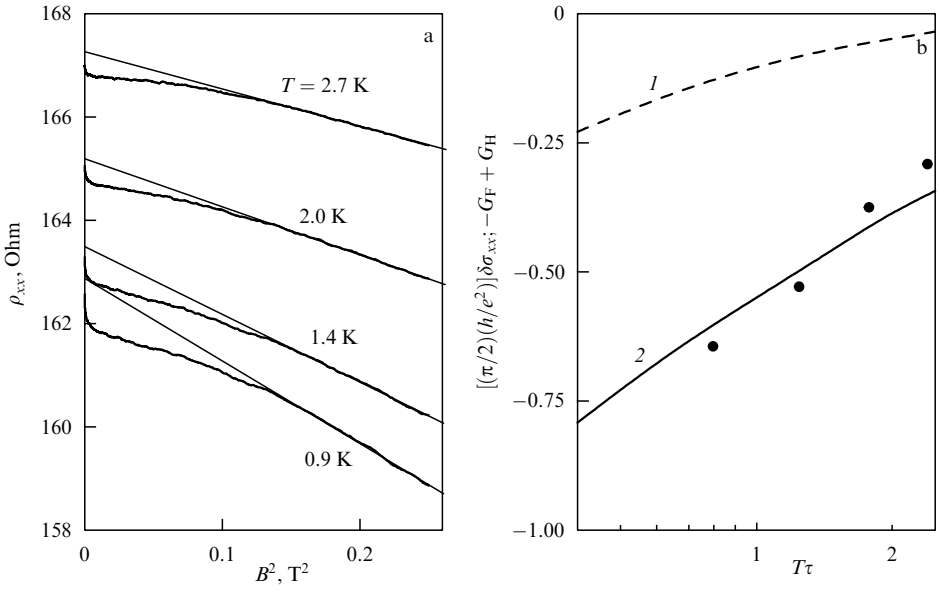

Figure 6. (a) Magnetoresistance as a function of B^2. (b) Experimentally determined correction $\Delta\sigma_{xx}^{ee}(T)$ (dots) and theoretical dependences for it: curve *1* — $F_0^\sigma = -0.15$, smoothly varying scattering potential; curve *2* — $F_0^\sigma = -0.16$, mixed scattering, $\gamma = 5$.

case of mixed scattering. In the latter case, a parameter γ is introduced to describe the relative contribution of each type of scattering [7]. It is seen that whereas assuming scattering by a long-period potential alone leads to disagreement with experiment, good agreement is obtained in the mixed scattering case. Thus, our analysis points to the correct description of scattering as a necessary condition for adequately describing interaction-induced corrections to conductivity — whether in a zero magnetic field or in strong magnetic fields leading to parabiotic magnetoresistance.

References

1. Lee P A, Ramakrishnan T V *Rev. Mod. Phys.* **57** 287 (1985)
2. Altshuler B L, Aronov A G, in *Electron-Electron Interactions in Disordered Systems* (Modern Problems in Condensed Matter Sciences, Vol. 10, Eds A L Efros, M Pollak) (Amsterdam: North-Holland, 1985) p. 1
3. Finkel'shtein A M *Zh. Eksp. Teor. Fiz.* **84** 168 (1983) [*Sov. Phys. JETP* **57** 97 (1983)]; *Pis'ma Zh. Eksp. Teor. Fiz.* **40** 63 (1984) [*JETP Lett.* **40** 796 (1984)]
4. Kravchenko S V et al. *Phys. Rev. B* **50** 8039 (1994)
5. Zala G, Narozhny B N, Aleiner I L *Phys. Rev. B* **64** 214204 (2001)
6. Zala G, Narozhny B N, Aleiner I L *Phys. Rev. B* **64** 201201 (2001)
7. Gornyi I V, Mirlin A D *Phys. Rev. Lett.* **90** 076801 (2003); *Phys. Rev. B* **69** 045313 (2004)
8. Gold A, Dolgopolov V T *Phys. Rev. B* **33** 1076 (1986)
9. Proskuryakov Y Y et al. *Phys. Rev. Lett.* **89** 076406 (2002)
10. Shashkin A A et al. *Phys. Rev. B* **66** 073303 (2002)
11. Kvon Z D et al. *Phys. Rev. B* **65** 161304 (2002)
12. Olshanetsky E B et al. *Phys. Rev. B* **68** 085304 (2003)
13. Renard V T et al. *Phys. Rev. B* **72** 075313 (2005)
14. Olshanetsky E B et al. *Europhys. Lett.* **71** 665 (2005)
15. Abrahams E et al. *Phys. Rev. Lett.* **42** 673 (1979)
16. Brunthaler G et al., cond-mat/0207170